Journal of Materials Chemistry A

COMMUNICATION

View Article Online
View Journal | View Issue

Cite this: J. Mater. Chem. A, 2017, 5, 97

# High sulfur loading lithium–sulfur batteries based on a upper current collector electrode with lithium-ion conductive polymers†

Received 23rd September 2016
Accepted 21st November 2016

DOI: 10.1039/c6ta08264e

www.rsc.org/MaterialsA

Yiyong Zhang, Kun Li, He Li, Yueying Peng, Yunhui Wang, Jing Wang and Jinbao Zhao*



We report an effective double current collector electrode. In this study, we achieve a high areal loading double current collector electrode with high areal capacity density and long cycle life. We also adjust the charging condition (constant capacity charging) which leads to long cycle life with almost no capacity fading.

The rapid development of emerging applications, including military power supplies, electric vehicles and energy storage systems for renewable sources, has placed higher demands on the energy density of batteries. High-energy-density energy storage devices with low cost are in urgent need for these applications. The lithium–sulfur (Li–S) battery with the features of a high theoretical specific energy density of 2600 W h $kg^{-1}$, low cost and nontoxicity is one of the most promising candidates.[1–6] However, its practical application is impeded by several problems, such as the high solubility and diffusivity of polysulfide intermediates, the low electronic conductivity of sulfur and its discharge product, volume expansion and the related side reaction caused by the shuttle effect.[7] The above factors lead to low sulfur utilization, low coulombic efficiency, fast capacity fade and short cycle life.[8,9] To circumvent these obstacles, all kinds of carbon–sulfur (C–S) composites have been prepared as active cathode materials, such as active carbon–S composites,[1,2,10] mesoporous C–S composites,[11,12] graphene–S composites,[13–17] carbon nanotubes–S composites[18–23] and hollow carbon nanofibers–S composites.[24] With these approaches, many researchers have been able to achieve excellent cycling performance. However, the excellent cycling performance is achieved with low areal loading sulfur cathodes (usually <2.0 mg $cm^{-2}$). It is difficult, even it may not be possible at all, to attain the real energy-density potential of Li–S batteries with these low areal loading electrodes.

Recently, Li *et al.*[25] proposed that we should search for the rational design and synthesis of various hollow micro-/nanostructures with controlled shapes, tailored shell structures and designed chemical compositions for advanced Li–S batteries in the future. Various configurations have been considered as an alternative approach to increase the areal loading of sulfur electrodes and reduce the shuttle effect.[26–32] Many advanced interlayers, which are fabricated from microporous carbon,[26] carbon nanotubes,[27] carbon nanofibers,[28] and graphene oxide,[29] have been inserted between the separator and cathode, which can trap the soluble polysulfides and greatly decrease the charge transfer resistance, resulting in a better utilization efficiency of the active materials and improved cyclability of the batteries. In addition, Ren and co-workers utilized a three-dimensional hybrid graphene network as a current collector to attain a "double high" sulfur electrode with 9.8 mg $cm^{-2}$ areal loading and 83 wt% sulfur content.[30] Li *et al.* also reported a 'pie' structured electrode, which provided an excellent balance between gravimetric and areal energy densities. The free-standing paper electrode (S mass loading: 3.6 mg $cm^{-2}$) delivered a high specific capacity of 1314 mA h $g^{-1}$ (4.7 mA h $cm^{-2}$) at 0.1C (0.6 mA $cm^{-2}$) accompanied by good cycling stability.[31] Zhang's group fabricated free-standing carbon nanotube@sulfur paper electrodes which were able to achieve ultrahigh sulfur loading ranging from 6.3 to 17.3 mg $cm^{-2}$.[32] Manthiram *et al.* reported a robust, ultra-tough, flexible cathode with the active-material fillings encapsulated between two buckypapers (B), which suppressed the irreversible polysulfide diffusion to the anode and offered excellent electrochemical reversibility with a low capacity fade rate of 0.06% per cycle after 400 cycles. It showed an areal capacity of as high as 5.1 mA h $cm^{-2}$, which increased further to approach 7 mA h $cm^{-2}$ on coupling with carbon-coated separators.[33] However, almost all of the high areal loading sulfur electrodes (>4.0 mg $cm^{-2}$) reported are aluminum-foil-free, and such "free standing" electrodes are not applicable for industrial

*State Key Lab of Physical Chemistry of Solid Surfaces, Collaborative Innovation Center of Chemistry for Energy Materials, College of Chemistry and Chemical Engineering, Xiamen University, Xiamen 361005, P. R. China. E-mail: jbzhao@xmu.edu.cn; Fax: +86-592-2186935; Tel: +86-592-2186935*

† Electronic supplementary information (ESI) available. See DOI: 10.1039/c6ta08264e

production due to a high implementation cost. Therefore, Manthiram *et al.* recently developed blade-cast sulfur electrodes, and cells fabricated with this blade-cast sulfur electrode and an upper modified carbon-paper current collector. Benefiting from the unique pure sulfur electrode and an upper current collector design, the pure sulfur electrode displays low polarization, high sulfur utilization, and promising cycling stability even with an ultrahigh sulfur loading. A high areal capacity of 19.2 mA h $cm^{-2}$ has been achieved. A facile pure sulfur electrode strategy was demonstrated to increase the areal loading of blade-cast sulfur electrodes and improve the electrochemical performances of thick sulfur electrodes with consideration for scale-up in practical and commercial applications.[34]

Here, we report a double current collector electrode (this electrode is referred to as Al–S–VGCF), using Al foil as the under current collector, and forming a high areal loading pure sulfur electrode by using commercial sulfur powder directly as the active material *via* a blade-casting method, and then coating a layer of VGCF with the critical component of polyethylene oxide (PEO) as the upper current collector. Compared to the conventional electrode configuration, the Al foil and VGCF layer next to the sulfur layer can act as double current collectors from top to bottom to accelerate electron transport into the sulfur layer, while they can also serve as physical barriers to buffer the volume change during cycling, prevent active material exfoliation and thus maintain the integrity of the whole electrode. Moreover, the upper current collector VGCF layer with the critical component of PEO works as an effective reservoir to trap the dissolved polysulfides within the cathode region, without affecting the lithium ion diffusion, leading to suppression of the shuttle effect and improved long-lasting cycling stability. Finally, a high areal loading sulfur electrode could be achieved with high areal capacity density and long cycle life with a low implementation cost that might be applicable for industrial production. Our present work may open up a feasible and effective concept of using lithium-ion conductive polymers as a promising class of materials to build current collectors for better Li/S cells.

As shown in Scheme 1, the fabrication of the Al–S–VGCF electrode is quite facile. First, commercial sulfur powder (95 wt%) and poly(vinylidene fluoride) (PVDF, 5 wt%) binders were mixed and dispersed well in *N*-methyl-pyrrolidone (NMP), and then coated onto an Al foil substrate by using the doctor blade casting method to obtain the Al–S electrode. Through restricting the amount of NMP solvent and the thickness of the S layer, Al–S electrodes with different areal sulfur loadings could be obtained easily. Second, the commercial VGCF (90 wt%), PEO (5 wt%) and carboxy methylated cellulose (CMC, 5 wt%) binders were mixed and dispersed well in deionized water, and then coated onto the Al–S electrode to obtain the Al–S–VGCF electrode. Here, the VGCF layer serves as the upper current collector and the adsorption layer for the electrolyte and polysulfides; the negatively charged VGCF and PEO can prevent polysulfide diffusion by electrostatic repulsion without affecting the lithium ion diffusion; at the same time, the PEO gelled in the electrolyte can also prevent polysulfide diffusion by reducing the size of the pores of the VGCF layer.

The characterizations of VGCF are shown in Fig. S1.† We can see from Fig. S1a and b† that VGCF has a smooth surface and is uniformly distributed with a diameter of about 100 nm and

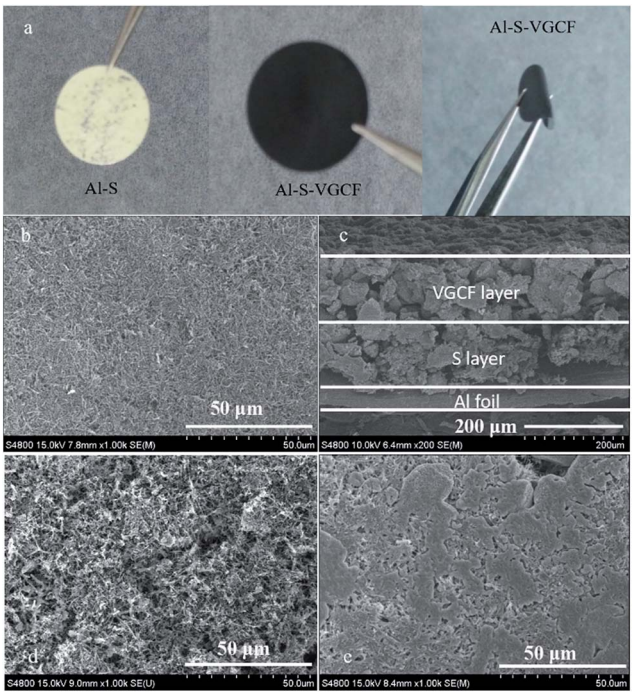


Fig. 1 (a) Apparent photographs of the Al–S electrode and Al–S–VGCF electrode. SEM images of (b) the surface of the Al–S–VGCF electrode (sulfur areal loading of ~5 mg $cm^{-2}$), (c) the cross-section of the Al–S–VGCF electrode (sulfur areal loading of ~5 mg $cm^{-2}$), (d) the surface of the Al–S–VGCF electrode with PEO after 100 cycles (sulfur areal loading of ~5 mg $cm^{-2}$), and (e) the surface of the Al–S–VGCF electrode without PEO after 100 cycles (charge state) (sulfur areal loading of ~5 mg $cm^{-2}$).


Scheme 1 Schematic of the fabrication of the Al–S–VGCF double current collector electrode.

 

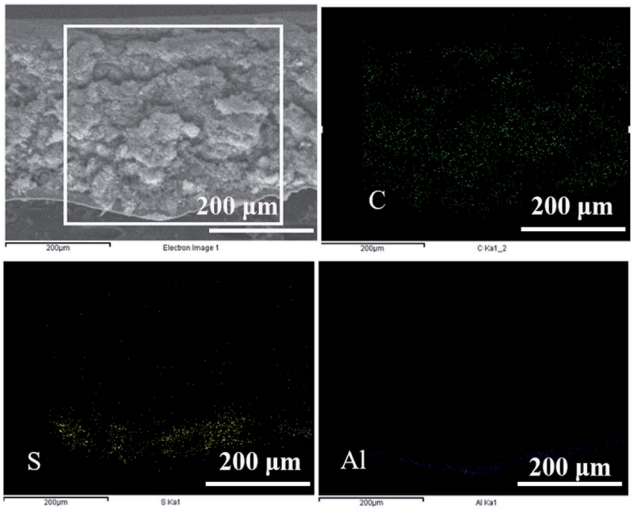


Fig. 2 Elemental mapping of the cross-section of the Al–S–VGCF electrode (sulfur areal loading of ~5 mg cm$^{-2}$).

a length of several μm. And from Fig. S1c and d† we can see that VGCF is graphitized carbon fiber. The optical photographs of the as-prepared Al–S and Al–S–VGCF electrodes are shown in Fig. 1a. The surface of the Al–S electrode is serrated. This facilitates intimate contact between the S layer and VGCF layer. The Al–S and Al–S–VGCF electrodes show excellent flexibility, strong adhesion and high mechanical strength. The surface of the VGCF layer shows an evenly and highly nanoporous structure with pore size around several hundred nanometers (Fig. 1b). The sandwich structure of the electrode can be further examined in the cross-sectional scanning electron microscope (SEM) image (Fig. 1c). The sulfur layer strongly adheres to the Al foil and VGCF layer as an integrated electrode. The thicknesses of the VGCF layer and the sulfur layer are about 100 μm and 100 μm, respectively. The sulfur layer strongly adheres to the Al foil and VGCF layer, and the loose structure of the VGCF layer and sulfur layer ensures that the liquid electrolyte penetrates easily into the whole sandwich structure, thus making the electrochemical reactions proceed. The elemental mapping results (Fig. 2) clearly confirm the layered Al–S–VGCF sandwich structure and further confirm that the VGCF layer is partially embedded in the sulfur layer. The weight ratio of the VGCF layer and the sulfur active material is around 1.

To demonstrate the effectiveness of the Al–S–VGCF double current collector electrode, a series of electrodes were prepared, with a range of areal sulfur loadings from ~2 mg cm$^{-2}$ to ~5 mg cm$^{-2}$. The electrochemical performances of the Al–S–VGCF electrodes are shown in Fig. 3. As shown in Fig. 3a, the discharge/charge curves show two distinct plateaus, confirming the excellent electrochemical reversibility of the Al–S–VGCF electrode with ultrahigh sulfur areal loading. The ultrahigh sulfur loading electrode delivers a stable discharge capacity of around 1100 mA h g$^{-1}$ at a current of 50 mA g$^{-1}$, which is about 65% of the theoretical capacity of sulfur (~1675 mA h g$^{-1}$). This further supports the idea that high sulfur utilization is possible by means of the integrated structure of the Al–S–VGCF double

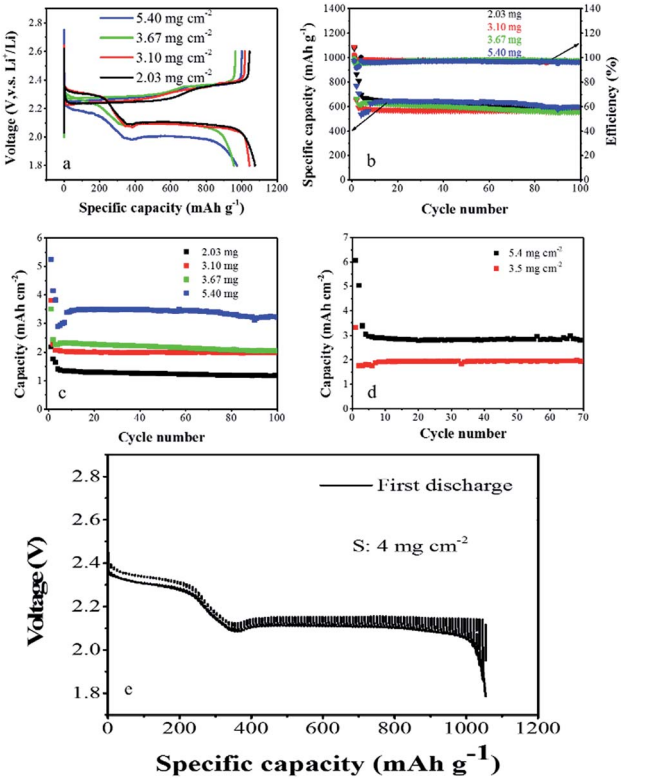


Fig. 3 Electrochemical performance of Li/(Al–S–VGCF) cells. (a) Discharge–charge profiles at a current density of 50 mA g$^{-1}$, (b) and (c) cycling performances at the first cycle at a current density of 50 mA g$^{-1}$ and after cycling at a current density of 100 mA g$^{-1}$, (d) discharge and charge at the first cycle at a current density of 50 mA g$^{-1}$ and after discharge and constant capacity charging at a current density of 100 mA g$^{-1}$, (e) GITT curves of the Al–S–VGCF electrode during the first discharge at a current density of 50 mA g$^{-1}$.

current collector electrode. Furthermore, the Al–S–VGCF electrodes show lower polarization compared to the conventional electrode. The charge–discharge potential difference of the cells with the Al–S–VGCF electrode remains almost constant under all conditions even when the sulfur areal loading was approximately 5 mg cm$^{-2}$. This indicates improved redox reaction kinetics and reversibility of the electrode. Surprisingly, from Fig. 3b we can see that all Al–S–VGCF electrodes show enhanced cycling stability and utilization efficiency of sulfur at a current of 100 mA g$^{-1}$. The mass specific capacities of all electrodes are around 650 mA h g$^{-1}$. And the coulombic efficiencies of all electrodes are around 97%. The excellent electrochemical performance of the ultrahigh areal loading Al–S–VGCF electrode is achieved. This is attributed to the integrated structure of the Al–S–VGCF double current collector electrode. The corresponding areal capacities of all Al–S–VGCF electrodes are shown in Fig. 3c. At a current of 100 mA g$^{-1}$, the areal sulfur loading ranges from ~2 mg cm$^{-2}$ to ~5 mg cm$^{-2}$; the corresponding areal capacities of all Al–S–VGCF electrodes are about 1.2 mA h cm$^{-2}$, 2.0 mA h cm$^{-2}$, 2.2 mA h cm$^{-2}$ and 3.4 mA h cm$^{-2}$, respectively. An areal capacity of more than 3 mA h cm$^{-2}$ is achieved when the areal sulfur loading is more than 5 mg cm$^{-2}$. The cell was first discharged/charged at 50 mA g$^{-1}$, and it

(the areal sulfur loading of 5 mg $cm^{-2}$) showed an areal capacity of as high as 5 mA h $cm^{-2}$. Considering the ultrahigh sulfur loading, these Al–S–VGCF electrodes show extraordinary cycling performance. We also adjust the charging condition (constant capacity charging) (the results are shown in Fig. 3d) which leads to long cycle life with almost no capacity fading because of the inhibition of electrochemical reactions along with severe polysulphide dissolution. To determine the electrochemical process of the Al–S–VGCF electrode, we used the galvanostatic intermittent titration technique (GITT). As shown in Fig. 3e, in the high-voltage region, the changes in voltages on removing the current remain small, demonstrating relatively fast electrode kinetics in this region. We have tested the rate performance of the Al–S–VGCF as shown in Fig. S2.† The rate performance of the high mass loading Al–S–VGCF electrode is relatively poor at high charge–discharge rates. This is because that the electrical conductivity and the $Li^+$ conductivity of the pure sulfur electrode are poor. The high-rate performance of the high mass loading Al–S–VGCF electrode needs to be further improved.

The excellent electrochemical performance of the Al–S–VGCF double current collector electrode can be attributed to its unique electrode structure. The highly conductive bottom current collector (Al foil) provides channels for electron transport, while the upper VGCF layer current collector serves as an electrolyte reservoir and physical trap for polysulfides (as shown in Fig. S3†). In addition, the negatively charged VGCF and PEO can prevent polysulfide diffusion by electrostatic repulsion; at the same time, the PEO gelled in the electrolyte can also prevent polysulfide diffusion by reducing the size of the pores of the VGCF layer. And we can see from the scanning electron microscopy (SEM) result shown in Fig. 1d and e and elemental mapping results shown in Fig. S4 and S5† that the surface of the VGCF layer with PEO and without PEO has no block reunion and block reunion after 100 cycles, revealing that PEO can prevent the sulfur species from reuniting, which is also critical for long-term cycling stability. In order to illustrate the importance of PEO to improve the electrochemical performance of Li–S batteries, we have investigated the cycling performance of Al–S–VGCF without PEO, and the result obtained is shown in Fig. S6.† We can see that the specific capacity of the electrode without PEO attenuates slowly after 40 cycles. Moreover, the PEO has shown a lot of excellent properties, such as good ionic conductivity and excellent mechanical properties as well as satisfactory electrochemical and interfacial stability.[35–37] The sufficient electron source combined with a large $Li^+$ supply by way of the electrolyte and PEO ensures conversion between $S_8$ and $Li_2S$.

In summary, we have successfully designed and fabricated a unique double current collector electrode consisting of the Al–S–VGCF sandwich structure by using the mature doctor-blade casting method. Benefiting from the unique double current collector electrode design, the Al–S–VGCF electrode shows high sulfur utilization and promising cycle stability even with ultrahigh areal sulfur loading. The Al–S–VGCF electrode demonstrates a high reversible specific capacity of ~650 mA h $g^{-1}$ and areal capacity of ~3 mA h $cm^{-2}$, and promising cycle stability even with an areal sulfur loading of ~5 mg $cm^{-2}$. We also adjust the charging condition (constant capacity charging) which leads to long cycle life with almost no capacity fading because of the inhibition of electrochemical reactions along with severe polysulphide dissolution. We believe that our results together with the simple and scalable feature of the electrode fabrication demonstrate that our electrode is highly promising for the development of high-energy-density Li–S batteries and has great promise in the commercial viability of Li–S batteries. And our present work may open up a feasible and effective concept of using lithium-ion conductive polymers as a promising class of materials to build current collectors for better Li/S cells.

## Acknowledgements

We gratefully acknowledge the financial support from the National Natural Science Foundation of China (Grant No. 21273185 and 21321062) and National Found for Fostering Talents of Basic Science (J1310024). The authors also wish to express their thanks to Prof. D. W. Liao for valuable suggestions.

## Notes and references

1 X. Ji, K. T. Lee and L. F. Nazar, *Nat. Mater.*, 2009, **8**, 500.
2 X. Ji, S. Evers, R. Black and L. F. Nazar, *Nat. Commun.*, 2011, **2**, 325.
3 A. Manthiram, Y. Z. Fu and Y. S. Su, *Acc. Chem. Res.*, 2013, **46**, 1125.
4 H. Wang, Y. Yang, Y. Liang, J. T. Robinson, Y. Li, A. Jackson, Y. Cui and H. Dai, *Nano Lett.*, 2011, **11**, 2644.
5 R. J. Chen, T. Zhao and F. Wu, *Chem. Commun.*, 2015, **51**, 18.
6 P. G. Bruce, S. A. Freunberger, L. J. Hardwick and J. M. Tarascon, *Nat. Mater.*, 2012, **11**, 19.
7 Y. Yang, G. Y. Zheng, S. Misra, J. Nelson, M. F. Toney and Y. Cui, *J. Am. Chem. Soc.*, 2012, **134**, 15387.
8 Q. Pang, J. Tang, H. Huang, X. Liang, C. Hart, K. C. Tam and L. F. Nazar, *Adv. Mater.*, 2015, **27**, 6021.
9 X. Liang, A. Garsuch and L. F. Nazar, *Angew. Chem., Int. Ed.*, 2015, **54**, 3907.
10 M. M. Rao, W. S. Li and E. J. Cairns, *Electrochem. Commun.*, 2012, **17**, 1.
11 J. Schuster, G. He, B. Mandlmeier, T. Yim, K. T. Lee, T. Bein and L. F. Nazar, *Angew. Chem., Int. Ed.*, 2012, **51**, 3591.
12 N. Jayaprakash, J. Shen, S. S. Moganty, A. Corona and L. A. Archer, *Angew. Chem., Int. Ed.*, 2011, **50**, 5904.
13 S. Lu, Y. Cheng, X. Wu and J. Liu, *Nano Lett.*, 2013, **13**, 2485.
14 W. D. Zhou, H. Chen, Y. C. Yu, D. L. Wang, Z. M. Cui, F. J. Disalvo and H. D. Abruña, *ACS Nano*, 2013, **7**, 8801.
15 G. Zhou, L. C. Yin, D. W. Wang, L. Li, S. Pei, F. Li and H. M. Cheg, *ACS Nano*, 2013, **7**, 5367.
16 L. Ji, M. Rao, L. Zhang, Y. Li, W. Duan, J. Guo, E. J. Cairns and Y. Zhang, *J. Am. Chem. Soc.*, 2011, **133**, 18522.
17 N. Li, M. Zheng, H. Lu, Z. Hu, C. Shen, X. Chang, G. Ji, J. Cao and Y. Shi, *Chem. Commun.*, 2012, **48**, 4106.
18 C. Wang, W. Wan, J. T. Chen, H. H. Zhou, X. X. Zhang, L. X. Yuan and Y. H. Huang, *J. Mater. Chem. A*, 2013, **1**, 1716.

 

19 F. Wu, J. Z. Chen, L. Li, T. Zhao and R. J. Chen, *J. Phys. Chem. C*, 2011, **115**, 24411.
20 L. X. Yuan, H. P. Yuan, X. P. Qiu, L. Q. Chen and W. T. Zhu, *J. Power Sources*, 2009, **189**, 1141.
21 S. Xin, L. Gu, N. H. Zhao, Y. X. Yin, L. J. Zhou, Y. G. Guo and L. J. Wan, *J. Am. Chem. Soc.*, 2012, **134**, 18510.
22 J. Guo, Y. Xu and C. Wang, *Nano Lett.*, 2011, **11**, 4288.
23 G. M. Zhou, D. W. Wang, F. Li, P. X. Hou, L. C. Yin, C. Liu, G. Q. Lu, I. R. Gentle and H. M. Cheng, *Energy Environ. Sci.*, 2012, **5**, 8901.
24 Z. Li, J. Zhang and X. W. Lou, *Angew. Chem., Int. Ed.*, 2015, **54**, 12886.
25 Z. Li, H. B. Wu and X. W. Lou, *Energy Environ. Sci.*, 2016, **9**, 3061.
26 Y. S. Su and A. Manthiram, *Nat. Commun.*, 2012, **3**, 1166.
27 Y. S. Su and A. Manthiram, *Chem. Commun.*, 2012, **48**, 8817.
28 J. Q. Huang, B. A. Zhang, Z. L. Xu, S. Abouali, M. A. Garakani, J. Q. Huang and J. K. Kim, *J. Power Sources*, 2015, **285**, 43.
29 X. F. Wang, Z. X. Wang and L. Q. Chen, *J. Power Sources*, 2013, **242**, 65.
30 G. Hu, C. Xu, Z. Sun, S. Wang, H. M. Cheng, F. Li and W. Ren, *Adv. Mater.*, 2016, **28**, 1603.
31 Z. Li, J. T. Zhang, Y. M. Chen, J. Li and X. W. Lou, *Nat. Commun.*, 2015, **6**, 8850.
32 Z. Yuan, H. J. Peng, J. Q. Huang, X. Y. Liu, D. W. Wang, X. B. Cheng and Q. Zhang, *Adv. Funct. Mater.*, 2014, **24**, 6105.
33 S. H. Chung, C. H. Chang and A. Manthiram, *Small*, 2016, **12**, 939.
34 L. Qie and A. Manthiram, *ACS Energy Lett.*, 2016, **1**, 46.
35 B. W. Zewde, S. Admassie, J. Zimmermann, C. S. Isfort, B. Scrosati and J. Hassoun, *ChemSusChem*, 2013, **6**, 1400.
36 B. W. Zewde, G. A. Elia, S. Admassie, J. Zimmermann, M. Hagemann, C. S. Isfort, B. Scrosati and J. Hassoun, *Solid State Ionics*, 2014, **268**, 174.
37 G. B. Appetecchi, J. Hassoun, B. Scrosati, F. Croce, F. Cassel and M. Salomon, *J. Power Sources*, 2003, **124**, 246.